

Structural Properties of Gd³⁺/Eu³⁺ Double Doped in Calcium Phosphate Glass System Based on “Huta Ginjang” Quartz Sand

Juniastel Rajagukguk¹, Jonny H. Panggabean², Juniar Hutahaean³, Howard Situmorang⁴, Elyzabeth Simanullang⁵

{juniastel@unimed.ac.id¹, gabejhp@gmail.com², junhut@unimed.ac.id³, howardstn@unimed.ac.id⁴, elisabetmanullang88@gmail.com⁵}

^{1,2,3,4,5}Department of Physics, Faculty of Mathematics and Natural Sciences, Universitas Negeri Medan, Medan 20221, Indonesia

Abstract. Quartz sand (Quartz Sand-QS) is an abundant natural material in Indonesia, specifically in Huta Ginjang, North Sumatra Province. This material has great potential as a basic material for the development of glass systems for medical imaging (X-ray imaging) applications. Synthesis and preparation of Huta Kidney quartz sand-based glass medium and di-double doped phosphate glasses with Gd³⁺ and Eu³⁺ ions (POCaGE) were performed for X-ray radiation scintillator applications. The composition of the glass system follows the chemical formula (15-x) QS-60P₂O₅-15CaO-5BaO-5Gd₂O₃-xEu₂O₃ (where x = 0; 0.5; 1.0; 1.5; 2.0 mol%). Samples were prepared using the melt-quenching technique at a melting temperature of 1200 °C and a glass system with good homogeneity and transparency was obtained. The structural properties of the glass medium were observed by using XRD and FTIR to find out the diffraction patterns and clustering of network functions in the glass structure. Based on the results of observations it is known that the quartz sand glass medium of Huta Kidney and calcium phosphate di-double doping with Gd³⁺/Eu³⁺ ions (POCaGE) has an amorphous structure which indicates that the properties of the medium after doped are intact as glass without any crystalline properties in it. In addition, the FTIR spectrum shows a variety of absorption bands, indicating the existence of functional bonds and clusters in the glass network.

Keywords: Glasses system; quartz sand; double doping Gd³⁺/Eu³⁺.

1 Introduction

Phosphate-based glasses have garnered significant attention in materials science due to their versatile properties, including low melting temperatures, high chemical durability, excellent optical transparency, and biocompatibility, making them suitable for applications ranging from nuclear waste storage to biomedical implants and optoelectronic devices [1]. Among

these, calcium phosphate glasses stand out for their ability to incorporate high concentrations of rare-earth (RE) ions, such as Gadolinium (Gd^{3+}) and Europium (Eu^{3+}) [2], which enhance their optical and luminescent properties. The incorporation of quartz sand (QS) as a primary component in glass formulations introduces a cost-effective and abundant resource, further expanding the potential for large-scale production [3]. This study introduces a novel calcium phosphate glass system based on quartz sand from Huta Ginjang, double-doped with Gd^{3+} and Eu^{3+} ions, with the chemical composition $(15-x) QS-60P_2O_5-15CaO-5BaO-5Gd_2O_3-xEu_2O_3$ (where $x = 0; 0.5; 1.0; 1.5; 2.0$ mol%). The aim is to investigate the structural and luminescent properties of this glass system, leveraged the synergistic effects of Gd^{3+} and Eu^{3+} co-doping to developed advanced materials for optoelectronic and radiation detection applications [4]. Phosphate glasses are characterized by a network of phosphate (P_2O_5), where P_2O_5 acts as the primary network former, creating a robust yet flexible structure. In the proposed composition, P_2O_5 serves as the backbone of the glass matrix, providing structural stability and enabling the incorporation of modifier ions [5]. Its high content ensures a strong covalent network, which is critical for maintaining the amorphous nature of the glass while accommodated high concentrations of Eu^{3+} ions [6-7].

Calcium Oxide functions as a network modifier, CaO also improves resistance to alkali solutions, making the glass suitable for harsh environmental conditions [8]. Barium oxide further modifies the glass network, BaO larger ionic radius compared to CaO contributes to a denser and more compact glass structure, enhancing mechanical properties and optical clarity. [9] The unique properties of this glass system could lead to innovative applications in laser technology and radiation detection, harnessing the increased luminescence of the co-doping of Gd^{3+} and Eu^{3+} ions [10]. Quartz sand primarily composed of silica (SiO_2), is a novel addition to this glass system, served as a secondary network former alongside P_2O_5 [3]. The used of quartz sand from Huta Ginjang, a local resource, introduces an economically viable alternative to high-purity silica, reducing production costs while maintaining structural integrity [3, 11-12]. The incorporation of QS also enhances the glass's thermal stability and optical transparency, critical for optoelectronic applications [13-14]. The variable QS content (adjusted by the Eu_2O_3 concentration) allows for fine-tuning of the glass's structural and optical properties, providing [15] flexibility in tailoring the material for specific applications. The double doped of Gd^{3+} and Eu^{3+} ions, introduced via Gd_2O_3 and Eu_2O_3 (0,0; 0,5; 1,0;1,5; 2,0 mol%), respectively, is a key feature of this glass system. [16]. Gadolinium ions (Gd^{3+}) act as both a network modifier and a luminescent center, enhancing the glass's structural density and dielectric properties. Gd^{3+} ions are known for their ultraviolet (UV) emission at approximately 312 nm, attributed to the ${}^6P_{7/2} \rightarrow {}^8S_{7/2}$ transition, make them ideal for phototherapy lamps and UV-emitting devices.

Additionally, Gd^{3+} facilitates energy transfer to co-doped ions, such as Eu^{3+} , amplified their luminescence efficiency. [17-19]. Europium ions are widely recognized for their intense red emission, particularly the ${}^5D_0 \rightarrow {}^7F_2$ transition at ~615 nm, which is hypersensitive to the local environment and ideal for applications in solid-state lighted and display devices. The co-doping strategy leverages the energy transfer from Gd^{3+} to Eu^{3+} , enhanced the overall luminescence intensity and enabled tunable emission properties by varied the Eu^{3+} concentration [20-21]. The novelty of this research lies in the integration of quartz sand from Huta Ginjang into a calcium phosphate glass system, combined with the strategic double doped of Gd^{3+} and Eu^{3+} ions [22-23]. While phosphate glasses doped with Eu^{3+} ions have been

extensively studied, the use of locally sourced quartz sand as a major component is unprecedented, offering a sustainable and cost-effective approach to glass synthesis [24-25].

The specific composition $(15-x)\text{QS}-60\text{P}_2\text{O}_5-15\text{CaO}-5\text{BaO}-5\text{Gd}_2\text{O}_3-x\text{Eu}_2\text{O}_3$ (where $x = 0; 0.5; 1.0; 1.5; 2.0$ mol%) allows for systematic investigation of the interplay between QS content and Eu^{3+} concentration, providing insights into the structural and luminescent behavior of the glass. The double-doped strategy, coupled with the unique properties of QS, positions this glass system as a promising candidate for advanced optoelectronic applications, including white light-emitted diodes (WLEDs), X-ray scintillators, and radiation shielded materials [26-28]. Recent research on Eu^{3+} doped phosphate glasses provides a foundation for this study. For instance, investigations into Gd^{3+} doped phosphate glasses have demonstrated increased density and UV emission intensity with higher Gd_2O_3 content, alongside improved structural rigidity. Similarly, Eu^{3+} -doped borate and boro-phosphate glasses have shown enhanced red emission with increased Eu^{3+} concentration, attributed to covalent Eu-O bonding [29-30]. [31] Studies on co-doped systems, such as $\text{Tb}^{3+}/\text{Eu}^{3+}$ in silicate sol-gel glass-ceramics, have reported energy transfer mechanisms that enable tunable luminescence, supporting the potential of $\text{Gd}^{3+}/\text{Eu}^{3+}$ co-doping. Additionally, research on calcium phosphate glasses doped with Dy^{3+} has highlighted their potential for X-ray imaging and temperature sensing, with efficient energy transfer from Gd^{3+} to Dy^{3+} . However, these studies primarily focus on conventional glass formers like B_2O_3 or SiO_2 , without exploring the use of natural quartz sand or the specific $\text{Gd}^{3+}/\text{Eu}^{3+}$ co-doping in a QS-based calcium phosphate matrix. [32-33]. The structural properties of phosphate glasses are influenced by the incorporation of Eu^{3+} ions, which act as network modifiers, induced depolymerization of the glass network. Fourier Transform Infrared (FTIR) spectroscopy studies have shown that Gd^{3+} ions increase the formation of NBOs, while Eu^{3+} ions enhance the covalency of the glass matrix, affecting optical properties like refractive index and bandgap [34-35].

Furthermore, the luminescent properties of $\text{Gd}^{3+}/\text{Eu}^{3+}$ co-doped glasses are anticipated to exhibit enhanced emission due to energy transfer, similar to that observed in Dy^{3+} -doped gadolinium calcium phosphate glasses. These findings underscore the potential of the proposed glass system to achieve superior optical and structural performance. This study addresses critical gaps in the literature by exploring the synergistic effects of $\text{Gd}^{3+}/\text{Eu}^{3+}$ co-doping in a quartz sand-based calcium phosphate glass. The use of Huta Ginjang quartz sand not only reduces reliance on high-purity silica but also aligns with sustainable material Potential applications include high-efficiency WLEDs, where tunable white light emission is achieved through $\text{Gd}^{3+}/\text{Eu}^{3+}$ energy transfer, and X-ray scintillators, where the high density and luminescence of Gd^{3+} -doped glasses enhance detection efficiency. Additionally, the glass's biocompatibility and chemical durability make it a candidate for biomedical applications, such as drug delivery systems or imaging agents. The study highlights the innovative use of locally sourced quartz sand, which not only provides economic benefits but also improves the optical and structural properties of the resulting calcium phosphate glass system.

2 Method

Glass with the chemical composition $(15-x) \text{QS}-60\text{P}_2\text{O}_5-15\text{CaO}-5\text{BaO}-5\text{Gd}_2\text{O}_3-x\text{Eu}_2\text{O}_3$ (where $x = 0; 0.5; 1.0; 1.5; 2.0$ mol%). was produced using high-purity chemicals (99.9%). However, quartz sand (QS) is known to contain 99% SiO_2 . The materials were weighed according to the glass composition calculations, then mixed homogeneously in an alumina container, and stored in a jar contained silica gel to reduce moisture in the materials. The homogenized mixture of materials is placed in a furnace and melted at a temperature of 1200°C for approximately 3 hours until a homogeneous molten glass is formed. After that, the molten glass is poured into a stainless steel mold, and the sample is annealed at a temperature of 500°C for 3 hours. The resulted glass is then cut into pieces measured $1\text{ cm} \times 0.3\text{ cm} \times 1.5\text{ cm}$.

3 Result and Discussion

3.1 Glass Pattern

The physical form of the glass medium is considered to play a very important role, so the shape of the glass is regarded as a crucial factor in the fabrication process. The glass used is selected based on criteria of very high transparency, good material homogeneity, and freedom from cracks or surface defects. Cut and polish are carried out to ensure optimal quality at the fabrication stage. The fabrication process of the glass, both before and after the cutting and polishing stages, can be observed in Figure 1, where the condition of the glass medium after cut and polishing show in Figure 2.



Figure 1. POCaGE glass samples before cut and polished



Figure 2. POCaGE glass samples after cut and polished

3.2 Physical Properties

The physical attributes that characterize the POCaGE glass medium comprise a diverse array of critical parameters, which include, but are not restricted to radius, the spatial distance between the cores, electric field strength, dielectric permittivity, molar refractivity, ionic polarizability criteria for metallization, and the measurable outcomes pertaining to reflection loss. All of these elements are meticulously and thoroughly elucidated within the scope of Table 1.

Table 1. Physical properties calculation of glass medium (15-x) QS-60P₂O₅-15CaO-5BaO-5Gd₂O₃-xEu₂O₃ (with x= 0; 0.5; 1.0; 1.5 and 2.0 mol%)

Measurement parameters	Glass Samples				
	POCaGE 0.0	POCaGE 0.5	POCaGE 1.0	POCaGE 1.5	POCaGE 2.0
Weight molar, M (g)	128.381	129.840	131.299	132.75 9	134.21 8
Density (g/cm ³)	2.838	2.864	2.909	2.921	2.951
Molar volume (cm ³ /mol)	45.231	45.330	45.129	45.451	45.481
Ion concentration, $N \times 10^{20}$ (ion/cm ³)	-	0.664	1.330	1.990	2.650
Polaron radius $\times 10^{-8}$ (Å)	-	9.950	7.880	6.900	6.270
Inter nuclear distance $\times 10^{-7}$	-	2.470	1.960	1.710	1.560
Field strength, $F \times 10^{16}$ cm ²	-	0.596	0.949	1.240	1.500
Refractive index (n)	1.539	1.541	1.543	1.546	1.570
Molar refractivity (R _m)	14.182	14.244	14.229	14.396	14.930
Molar electronic Polarization $\times 10^{-24}$	5.630	5.650	5.640	5.710	5.920
Metallization Criteria (M)	0.686	0.685	0.685	0.683	0.672
Reflection loss (R) %	4.515	4.533	4.562	4.602	4.924
Dielectric constant (ε)	2.370	2.375	2.382	2.391	2.466

Table 1 shows that the physical properties of the glass medium are influenced by the addition of Europium ions. Density is considered one of the important parameters in determining glass quality, where density measurements were conducted using the Archimedes method with the glass medium submerged in water [36]. Density, refractive index, ion concentration, reflection loss and dielectric constant have shown an increasing trend with the increase in Eu³⁺ ion concentration [37]. The increase in molar weight is due to the decrease in Quartz Sand (QS) as the amount of Eu₂O₃ increases, since Eu₂O₃ has a higher molar mass than QS [38]. The polaron radius and inter nuclear distance decrease as the concentration of RE ions increases, indicating a reduction in free space and a more compact glass structure. The material exhibited insulating behavior with metallization; however, in this study, the average value is approximately 0.685. Generally, values closer to zero suggest conductivity, while those nearer to one indicate insulation.

3.3 Structural Properties

X-ray diffraction (XRD) is widely used as an analytical technique for the characterization of sample structures. The POCaGE glass spectrum displayed in Figure 3 is shown within the range of 10° to 90°, where the spectrum shape is observed to align with previous research conducted by [39], and no sharp peaks are found throughout the observed 2θ diffraction angle region. The XRD data, which exhibits non-sharp diffraction peaks but broad humps observed at around the 2θ angle, has been utilized to indicate the characteristics of an amorphous material [40]. A wide scattering at low angles is noted, which is a typical feature of structural disorder. This suggests that all prepared samples possess an amorphous structure, a

characteristic of glass materials. Thus, it can be concluded that all prepared samples are glass materials with an amorphous structure. This condition is believed to be caused by the glass composition being perfectly melted in the furnace and the homogeneous mixing of the chemical composition.

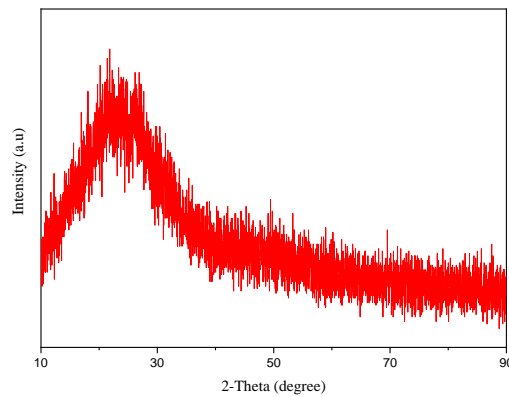


Figure 3. XRD spectra of POCaGE1.5 glasses

3.4 Optical Properties

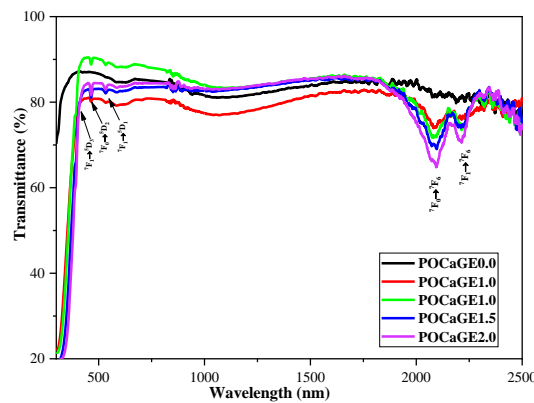


Figure 4. Transmittance Spectra of Eu^{3+} doped QS- P_2O_5 -CaO-BaO- Gd_2O_3 - Eu_2O_3

The Transmittance Spectra of Eu^{3+} doped QS- P_2O_5 -CaO-BaO- Gd_2O_3 - Eu_2O_3 glass are shown in the Figure 4 transmittance indicates how much light passes through a material higher values signify greater transparency [41]. All samples exhibit a sharp increase in transmittance below 400 nm, peaking and stabilizing in the 500–2000 nm range. [42] Variations in POCaGE composition affect transparency levels, with maximum transmittance reaching 70–90% in the visible to near-infrared range [43]. A slight decrease in transmittance occurs beyond 2000 nm due to characteristic absorption of the glass or impurities in the infrared band. The cut-off wavelength, marking the transition from opaque to transparent behavior, occurs around 350–400 nm. Below this range, transmittance is very low due to significant light absorption. Beyond the cut-off wavelength, the glass becomes sufficiently transparent for optical applications, such as optical media or transparent filters [44].

The absorption coefficient $\alpha(\nu)$ was calculated from the absorbance (A) using the following equation:

$$\alpha(\nu) = \left(\frac{1}{d}\right) \ln\left(\frac{I_0}{I}\right) = 2.303 \left(\frac{A}{d}\right)$$

where A is the absorbance at frequency ν and d is the thickness of the sample. For an absorption by an indirect transition, the equation takes the form:

$$E_{opt} = h\nu - \left(\frac{h\nu}{B}\right)^{1/2}$$

where B is a constant called band tailing parameter, $h\nu$ is the incident photon energy and E_{opt} is the optical band gap energy. Using the above equations, by plotting $(ah\nu)^{1/2}$ as a function of photon energy $h\nu$, one can find the optical band gap energy (E_{opt}) for indirect transitions and direct by extrapolating the linear region of the curve to the $h\nu$ axis [45] and are shown in Figure 5.

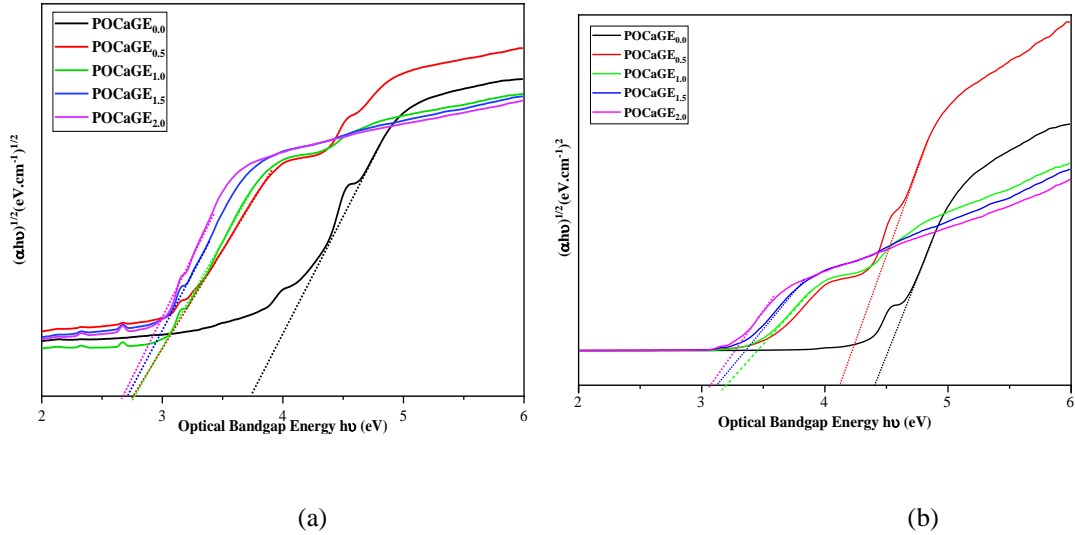


Figure 5. (a) Indirect and (b) Direct optical band gap of POCaGE glass samples

Table 2. Direct and indirect optical band gaps of the various glass samples

Glass samples	Indirect (eV)	Direct (eV)
POCaGE0.0	3.75	4.46
POCaGE0.5	2.78	4.17
POCaGE1.0	2.77	3.28
POCaGE1.5	2.72	3.21
POCaGE2.0	2.67	3.15

4 Conclusion

Europium-doped phosphate glasses were successfully synthesized via the melt-quenching technique and characterized using various spectroscopic methods, including X-ray diffraction (XRD) and Fourier Transform Infrared (FTIR) spectroscopy. The results confirm that the prepared samples exhibit complete amorphous nature, as evidenced by the absence of crystalline peaks in XRD patterns. Physical properties such as density, refractive index, reflection loss, and dielectric constant demonstrated a consistent increasing trend with rising Eu^{3+} ion concentration, reflecting enhanced ion packing and network modifications. Structurally, Eu^{3+} ions act as network modifiers in the phosphate glass matrix, promoting depolymerization and the formation of non-bridging oxygens (NBOs), as revealed by FTIR analysis. These findings highlight the potential of Eu^{3+} -doped phosphate glasses for applications in optical and luminescent devices, warranting further exploration of their luminescent efficiency and stability.

References

- [1] Arafat, A., Samad, S. A., Wadge, M. D., Islam, T., Lewis, A. L., Barney, E. R., & Ahmed, I. (2020). Thermal and crystallization kinetics of yttrium-doped phosphate-based glasses. *International Journal of Applied Glass Science*. <https://doi.org/10.1111/IJAG.14163>
- [2] Meejitpaisan, P., Insiripong, S., Kedkaew, C., Kim, H. J., & Kaewkhao, J. (n.d.). Radioluminescence and optical studies of gadolinium calcium phosphate oxyfluoride glasses doped with Sm^{3+} . <https://doi.org/10.1016/j.radphyschem.2016.01.043>
- [3] Sukach, M. (2023). Quartz sand is an affordable inexpensive raw material for technologies of electronics and photovoltaics. *Pìdvodnì Tehnologii*. <https://doi.org/10.32347/uwt.2022.12.1801>
- [4] Saha, S., Ntarisa, A. V., Quang, N. D., Kim, H. J., Kothan, S., & Kaewkhao, J. (2022). Synthesis and elemental analysis of gadolinium halides (GdX_3) in glass matrix for radiation detection applications. *Optical Materials*. <https://doi.org/10.1016/j.optmat.2022.112490>
- [5] Carta, D., Foroutan, F., Kyffin, B. A., Abrahams, I., Corrias, A., Gupta, P., Velliou, E., & Knowles, J. C. (2020). Mesoporous Phosphate-Based Glasses Prepared via Sol-Gel. *ACS Biomaterials Science & Engineering*. <https://doi.org/10.1021/ACSBIOMATERIALS.9B01896>
- [6] Liao, K., Masuno, A., Inoue, H., & Mizoguchi, T. (2020). Nano-meter Scale Observation of Local Network Structure in Aluminosilicate Glass via Vibrational EELS. *Microscopy and Microanalysis*. <https://doi.org/10.1017/S143192762001644X>
- [7] Tasik, R. B. (2023). Redox Reactions in Glasses. *Advances in Material Research and Technology*. https://doi.org/10.1007/978-3-031-20266-7_2
- [8] Olivier, M. (2023). The intrinsic role of network modifiers (Ca versus Mg) in the reaction kinetics and microstructure of sodium silicate-activated $\text{CaO-MgO-Al}_2\text{O}_3\text{-SiO}_2$ glasses. *Cement and Concrete Research*. <https://doi.org/10.1016/j.cemconres.2022.107058>
- [9] Kolahi, A. (2022). Mechanical properties, bioactivity and cell behavior of barium-containing calcium-phospho-alumino-borosilicate glass. *Ceramics International*. <https://doi.org/10.1016/j.ceramint.2021.11.309>

- [10] Wantana, N., Kaewnuam, E., Chanlek, N., Kim, H.-J., & Kaewkhao, J. (2023). Influence of Gd³⁺ on structural and luminescence properties of new Eu³⁺-doped borate glass for photonics material. *Radiation Physics and Chemistry*. <https://doi.org/10.1016/j.radphyschem.2023.110812>
- [11] Liu, L., Shao, W., Liu, L., Wang, S., & Zhang, L. (2020). *Quartz sandstone high-value comprehensive utilization method*.
- [12] Du, J. (2020). *High-purity quartz sand and production process thereof*.
- [13] Sarumaha, C. S., Rajagukguk, J., Tongdang, J., Chanthima, N., Kim, H. J., Kothan, S., & Kaewkhao, J. (2023). *Effect of Gd₂O₃ in Li₂O-AlF₃-CaF₂-P₂O₅-Eu₂O₃ glasses for laser medium and X-rays detection material applications*.
- [14] Zhou, Y. (2023). Quasilocalized vibrational modes as efficient heat carriers in glasses. *International Journal of Heat and Mass Transfer*. <https://doi.org/10.1016/j.ijheatmasstransfer.2023.124150>
- [15] Wantana, N., Kaewnuam, E., Chanthima, N., Kim, H. J., & Kaewkhao, J. (2022). Tuneable luminescence of Pr³⁺-doped sodium aluminium gadolinium phosphate glasses for photonics applications. *Optik*. <https://doi.org/10.1016/j.ijleo.2022.169668>
- [16] Rajagukguk, J., Rajagukguk, D. H., Syahputra, R. A., Fibriasari, H., Sarumaha, C., Kirdsiri, K., Kothan, S., & Kaewkhao, J. (Eds.). (2024). Radioluminescence properties of huta ginjang quartz sand doped with CeF₃ and Tb₂O₃ for scintillator application. *Radiation Physics and Chemistry*, 223. <https://doi.org/https://doi.org/10.1016/j.radphyschem.2024.111939>
- [17] Ullah, I., Sarumaha, C. S., Angnanon, A., Khan, I., Shoaib, M., Khattak, S. A., Kothan, S., Sangwanateee, N., Rooh, G., & Kaewkhao, J. (2022). Spectral features of Gd₂O₃ modified Sm³⁺ doped lithium strontium borate glasses for solid-state laser applications. *Ceramics International*. <https://doi.org/10.1016/j.ceramint.2022.12.255>
- [18] Zagrai, M., Macavei, S., Rada, S., Pică, M. E., & Pruneanu, S. (2022). Structural and spectroscopic properties of gadolinium-lead-lead dioxide glasses. *Journal of Non-Crystalline Solids*. <https://doi.org/10.1016/J.JNONCRY SOL.2021.121234>
- [19] Aliyu, A. M. (2019). *Structural, optical and Judd-Ofelt parameters study on samarium and dysprosium ions doped calcium sulfate and magnesium sulfate ultra-phosphate glasses*.
- [20] Riyas, K. M., Prasannan, P., & Jayaram, P. (2020). Multiple deep-level defect correlated emissions and phosphorescence in Eu³⁺ doped Gd₂O₃ compound systems. *Materials Letters*. <https://doi.org/10.1016/J.MATLET.2020.127925>
- [21] Al Abboodi, M. A. N. (2022). Luminous tuning in Eu³⁺/Mn⁴⁺ co-doped double perovskite structure by designing the site-occupancy strategy for solid-state lighting and optical temperature sensing. *Materials Research Bulletin*. <https://doi.org/10.1016/j.materresbull.2021.111704>
- [22] Botia, S. (2022). Synthesis and optical properties of novel Gd³⁺-doped BaZn₂(PO₄)₂ glass-ceramics for radiation detection applications. *Journal of Rare Earths*. <https://doi.org/10.1016/j.jre.2021.11.010>
- [23] Rajagukguk, J., Simamora, P., Sitingjak, L., Simanullang, E., Sarumaha, C., Intachai, N., & Kothan, S. (Eds.). (2025). NIR luminescence properties of Nd³⁺ ion doped glasses medium based on Huta Ginjang quartz sand. *Radiation Physics and Chemistry*, 229. <https://doi.org/https://doi.org/10.1016/j.radphyschem.2024.112466>
- [24] Gupta, S. K., Tripathy, S., Bharti, D., Pal, S. K., Verma, S., Pal, K., & Ray, S. S. (2023). One pot synthesis of phosphate glass with in situ formed nanodiamonds from adenosine triphosphate for bone repair. *Ceramics International*. <https://doi.org/10.1016/j.ceramint.2023.04.089>

- [25] Liu, Q., Feng, L., Sun, Y., Fang, S., Zhang, Z., Han, N., Wang, J., Zhang, C., & Wang, T. (2022). Effects of phosphate glass on Cs⁺ immobilization in geopolymer glass-ceramics. *Ceramics International*. <https://doi.org/10.1016/j.ceramint.2022.10.113>
- [26] Wang, Z., Li, J., Huang, F., Hua, Y., Tian, Y., Zhang, X., & Xu, S. (2023). Multifunctional Optical Materials Based on Transparent Inorganic Glasses Embedded with PbS QDs. *Journal of Alloys and Compounds*. <https://doi.org/10.1016/j.jallcom.2023.169040>
- [27] Cajko, K. O., Dimitrievska, M., Dimitrievska, M., Dimitrievska, M., Sekulić, D. L., Petrović, D. M., & Lukić-Petrović, S. R. (2021). Ag-doped As–S–Se chalcogenide glasses: a correlative study of structural and dielectrical properties. *Journal of Materials Science: Materials in Electronics*. <https://doi.org/10.1007/S10854-021-05384-W>
- [28] Huang, P.-Z., Chen, B., Xia, D., Li, Z., Zhang, B., Liu, Z., Wei, D., Li, Z., & Liu, J. H. (2023). Integrated Reconfigurable Photon-Pair Source Based on High-Q Nonlinear Chalcogenide Glass Microring Resonators. *Nano Letters*. <https://doi.org/10.1021/acs.nanolett.3c00858>
- [29] Wantana, N., Kaewnuam, E., Damdee, B., Kaewjaeng, S., Kothan, S., Kim, H. J., & Kaewkhao, J. (2018). Energy transfer based emission analysis of Eu³⁺ doped Gd₂O₃-CaO-SiO₂-B₂O₃ glasses for laser and X-rays detection material applications. *Journal of Luminescence*. <https://doi.org/10.1016/J.JLUMIN.2017.10.004>
- [30] Ramakrishna, P. V., Padhi, R. K., Mohapatra, D., Jena, H., & Panigrahi, B. K. (2022). Structural characterization, Gd³⁺ → Eu³⁺ energy transfer and radiative properties of Gd/Eu in codoped Li₂O–ZnO–SrO–B₂O₃–P₂O₅ glass. *Optical Materials*. <https://doi.org/10.1016/j.optmat.2022.112060>
- [31] Kirdsiri, K., & Gan, Z. (2022). Physical and photoluminescence investigations of Eu³⁺ doped gadolinium borate scintillating glass. *Radiation Physics and Chemistry*. <https://doi.org/10.1016/j.radphyschem.2022.110386>
- [32] Li, W., Chen, Z., Zhao, P., & Fan, Y. (2021). Luminescence and energy transfer of color-tunable Tb³⁺/Sm³⁺-co-doped BaZn₂(PO₄)₂ glass-ceramic phosphors. *Optical Materials*. <https://doi.org/10.1016/J.OPTMAT.2021.111782>
- [33] Zeng, F., &)2022. (اسمندر م ي). Photochromic tuning and scintillation properties of Tb³⁺/Eu³⁺ co-doped calcium gadolinium zinc borosilicate glass. *Journal of Non-Crystalline Solids*. <https://doi.org/10.1016/j.jnoncrysol.2022.121705>
- [34] Rajagukguk, J., Rajagukguk, D. H., Gultom, R. S., Simamora, P., Situmorang, R., & Sarumaha, C. S. (2022). Structure and emission properties of Nd³⁺ doped oxyfluorophosphate glasses. *Journal of Physics: Conference Series*. <https://doi.org/10.1088/1742-6596/2193/1/012007>
- [35] Faleiro, J. H., Dantas, N. O., Silva, A. C. A., Barbosa, H. P., Torquato da Silva, B. H. S., Lima, K. de O., Gonçalves, R. R., & Ferrari, J. L. (2021). Niobium oxide influence in the phosphate glasses triply doped with Er³⁺/Yb³⁺/Eu³⁺ prepared by the melting process. *Journal of Non-Crystalline Solids*. <https://doi.org/10.1016/J.JNONCRY SOL.2021.121051>
- [36] Rajagukguk, J., Simamora, P., Sitinjak, L., Simanullang, E., Sarumaha, C. S., Intachai, N., & Kothan, S. (2025). NIR luminescence properties of Nd³⁺ ion doped glasses medium based on Huta Gijang quartz sand. *Radiation Physics and Chemistry*, 229, 112466.
- [37] Shoaib, M., Khan, I., Khan, S., Mukamil, S., Ifseisi, A. A., Assal, M. E., ... & Kaewkhao, J. (2024). Analysis of Eu³⁺-ions concentration effect on the spectral properties of zinc-barium-boron-tellurite glasses. *Indian Journal of Physics*, 1-8.
- [38] Chimalawong, P., Kaewkhao, J., Kedkaew, C., & Limsuwan, P. (2010). Optical and electronic polarizability investigation of Nd³⁺-doped soda-lime silicate glasses. *Journal of Physics and Chemistry of Solids*, 71(7), 965-970

- [39] Hutahaean, J., Tambunan, F. E. F., Rajagukguk, J., Sarumaha, C. S., & Kaewkhao, J. (2024, November). Quartz Sand “Huta Ginjang” On Physical Properties And Structure Of Phosphate Glass Medium. In *Journal of Physics: Conference Series* (Vol. 2908, No. 1, p. 012009). IOP Publishing.
- [40] Rajagukguk, J., Rajagukguk, D. H., Syahputra, R. A., Fibriasari, H., Sarumaha, C., Kirdsiri, K., Kothan, S., & Kaewkhao, J. (Eds.). (2024). Radioluminescence properties of huta ginjang quartz sand doped with CeF₃ and Tb₂O₃ for scintillator application. *Radiation Physics and Chemistry*, 223. <https://doi.org/https://doi.org/10.1016/j.radphyschem.2024.111939>
- [41] Rajagukguk, J., Simamora, P., Sitingjak, L., Simanullang, E., Sarumaha, C., Intachai, N., & Kothan, S. (Eds.). (2025). NIR luminescence properties of Nd³⁺ ion doped glasses medium based on Huta Ginjang quartz sand. *Radiation Physics and Chemistry*, 229. <https://doi.org/https://doi.org/10.1016/j.radphyschem.2024.112466>
- [42] Hu, H. (2023). Analysis of the Transmission Spectrum of Flat Glass from Near-infrared to the Ultraviolet. *Highlights in Science, Engineering and Technology*. <https://doi.org/10.54097/hset.v48i.8352>
- [43] Guo, X., Chen, H., Guo, H., Qin, Y., Zeng, Z., Fei, Q., Jian, Z., Chen, H., & Wang, G. (2024). Water-induced highly transparent SiO₂ porous ceramics with tunable visible transparency, anti-fogging and thermal insulation. *Ceramics International*. <https://doi.org/10.1016/j.ceramint.2024.02.024>
- [44] Takenaka, K., Takenaka, K., & Kawamoto, Y. (2000). Ultraviolet Transmission Characteristics of Calcium Meta Phosphate Glass. *Journal of the Ceramic Society of Japan*. https://doi.org/10.2109/JCERSJ.108.1254_210
- [45] Sarumaha, C. S., Rajagukguk, J., Tongdang, J., Chanthima, N., Kim, H. J., Kothan, S., & Kaewkhao, J. (2022). Effect of Gd₂O₃ in Li₂O–AlF₃–CaF₂–P₂O₅–Eu₂O₃ glasses for laser medium and X-rays detection material applications. *Radiation Physics and Chemistry*, 199, 110362